

## Nanostructuring perovskite oxides: The impact of SrTiO<sub>3</sub> nanocube 3D self-assembly on thermal conductivity.

Stephen R. Yeandel,<sup>a,b</sup> Marco Molinari,<sup>a,c</sup> and Stephen C. Parker<sup>\*,a</sup>

<sup>a</sup> Department of Chemistry, University of Bath, Claverton Down, Bath BA2 7AY, U.K.

<sup>b</sup> Department of Chemistry, Loughborough University, Loughborough, LE11 3TU, U.K.

<sup>c</sup> Department of Chemistry, University of Huddersfield, Queensgate, Huddersfield, HD1 3DH, United Kingdom

\*Corresponding Author: s.c.parker@bath.ac.uk

### Supporting Information

#### Methodology

**Lattice thermal conductivity.** The lattice thermal conductivity was calculated using the Green - Kubo method<sup>1,2</sup> as implemented in the LAMMPS code.<sup>3</sup> This method is efficient as it suffers less from finite size effects than alternative approaches and gives a thermal conductivity tensor as a result, with the advantage that only a single calculation is required for complex structures and thus more suitable for nanostructured materials.<sup>4</sup> The disadvantage is that the calculation of the error on the value of thermal conductivity is challenging when using the Green-Kubo method and is discussed in detail by McGaughey and Larkin.<sup>5</sup> In order to calculate the thermal conductivity, the heat-flux was numerically integrated to give the autocorrelation function, which is then averaged over a portion of the integral to reduce the noise in the thermal conductivity.<sup>6</sup> The value of thermal conductivity was averaged over a region of 'neck regime'<sup>7</sup> after a moving average over 17 fs was applied to remove the highest frequency oscillations. The neck regime occurs when the value for thermal conductivity plateaus and before statistical error begins to contribute significantly to the thermal conductivity. The start and finish of the neck regime changes significantly between materials, temperatures and nanostructures and is evaluated separately for each system, in each direction of the systems and at each temperature.

**Lattice dynamics calculations.** The total phonon density of states (PDOS) at the  $\Gamma$  point were evaluated using the PHONOPY code<sup>8,9</sup>. The PDOS at the  $\Gamma$  point was calculated using the 5 atom cubic cell with lattice parameters  $a = b = c = 3.88 \text{ \AA}$  and  $\alpha = \beta = \gamma = 90^\circ$ . The PDOS (Fig. SI3) reveals four distinct Longitudinal Optical modes (LO) at the  $\Gamma$  point (and those at zero frequency, corresponding to a translations of the entire lattice). Landry et al.<sup>10</sup> outline a criterion to determine whether a vibrational mode at the  $\Gamma$  point PDOS appears in the HFACF spectra. An equivalent approach is to calculate sum the non-mass weighted eigenvectors for each vibrational mode; should the sum not equal zero, then a peak is expected in the HFACF spectra. These vibrational modes correspond to optical phonons which are capable of scattering heat-carrying

acoustic phonons as indicated by McGaughey et al.<sup>11</sup> For practicality a dimensionless normalised eigenvector sum cutoff of 0.01 was applied to the PDOS to remove modes of extremely low intensity or which are non-zero due only to numerical error. This treatment of the PDOS allows us to compare the HFACF spectrum of SrTiO<sub>3</sub> and the PDOS (Fig. S13). We refer to the treated PDOS as PDOS for simplicity. The relative heights of the peaks in the PDOS were chosen to be equal to the sum of the eigenvectors and correlate well when the HFACF spectra are plotted on a logarithmic scale. As our PDOS contains only the optical phonon frequencies at the  $\Gamma$  point, for those modes that do not appear in the PDOS the heat-flux remains zero throughout the entirety of the vibration due to symmetry, whereas for the remaining modes the direction and magnitude of heat-flux oscillates with the periodicity of the mode. The heat-flux of the systems depends on both the energy of the atoms and their velocity according to the Green-Kubo equation and therefore most peaks in the HFACF spectra are also IR active modes as there will usually be an accompanying change in dipole with the vibration.

**Table S11.** Models used for the configurations of nanocubes and bulk oxides. Perfect Stacking (Pm-3m). X-Displacement configuration in the X direction of half a cube width relative to the neighbouring cube (Cmmm). XY-Displacement configuration in the XY plane of a quarter of a cube width relative to the neighbouring cube (I4/mmm). In brackets by the stoichiometry of the surface.

System	a x b x c	$\alpha \times \beta \times \gamma$	TiO2 units	SrO units	composition
Pm-3m[SrO]	70 Å x 70 Å x 70 Å	90° x 90° x 90°	4912	5776	Sr <sub>1.18</sub> TiO <sub>3.18</sub>
Pm-3m[TiO <sub>2</sub> ]	70 Å x 70 Å x 70 Å	90° x 90° x 90°	5800	4912	SrTi <sub>1.18</sub> O <sub>3.36</sub>
Cmmm[SrO]	78 Å x 70 Å x 70 Å	90° x 90° x 65°	4912	5776	Sr <sub>1.18</sub> TiO <sub>3.18</sub>
Cmmm[TiO <sub>2</sub> ]	78 Å x 70 Å x 70 Å	90° x 90° x 65°	5800	4912	SrTi <sub>1.18</sub> O <sub>3.36</sub>
I4/mmm[SrO]	78 Å x 70 Å x 78 Å	90° x 65° x 65°	4912	5776	Sr <sub>1.18</sub> TiO <sub>3.18</sub>
I4/mmm[TiO <sub>2</sub> ]	78 Å x 70 Å x 78 Å	90° x 65° x 65°	5800	4912	SrTi <sub>1.18</sub> O <sub>3.36</sub>
SrTiO <sub>3</sub>	46.90 Å x 46.90 Å x 46.90 Å	90° x 90° x 90°	1728	1728	SrTiO <sub>3</sub>
TiO <sub>2</sub> anatase	45.23 Å x 45.23 Å x 48.02 Å	90° x 90° x 90°	2880	-	TiO <sub>2</sub>
TiO <sub>2</sub> rutile	45.58 Å x 45.58 Å x 45.02 Å	90° x 90° x 90°	3000	-	TiO <sub>2</sub>
SrO	51.74 Å x 51.74 Å x 51.74 Å	90° x 90° x 90°	-	4000	SrO

**Table S12.** The potential model developed by Teter<sup>12</sup> with the interactions based on Buckingham potential forms between cations and anions.

Interaction	A (eV)	$\rho$ (Å)	C (eV×Å <sup>6</sup> )	Charge
O-O	1844.7458	0.3436	192.58	1.2
Sr-O	14566.637	0.2450	81.773	2.4
Ti-O	23707.909	0.1856	14.513	-1.2

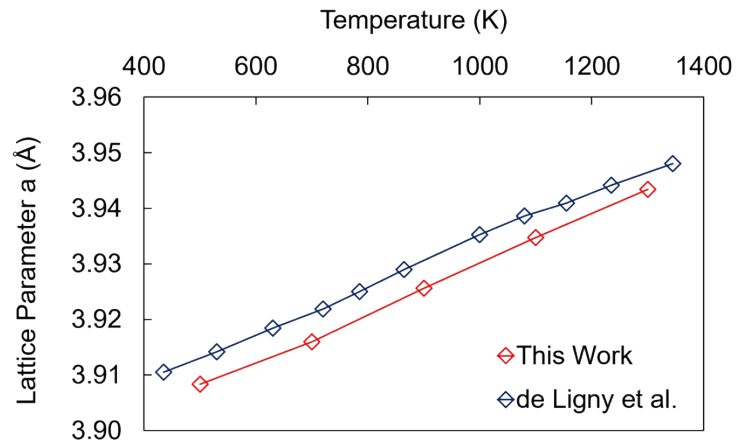


**Figure S11.** The calculated lattice vectors for SrTiO<sub>3</sub> as a function of temperature. The thermal expansion is the slope and was calculated to be  $1.13 \times 10^{-5} \text{ K}^{-1}$ , which compares well to the experimental thermal expansion of  $1.10 \times 10^{-5} \text{ K}^{-1}$  <sup>13</sup>.

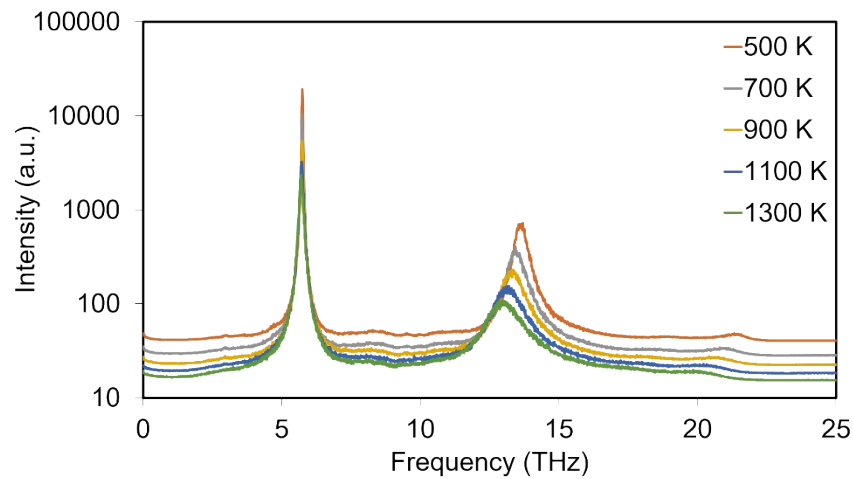


**Figure S12.** The Fourier transform of the heat-flux autocorrelation functions at different T of bulk SrTiO<sub>3</sub>, Log10 scale. Intensity in arbitrary units.

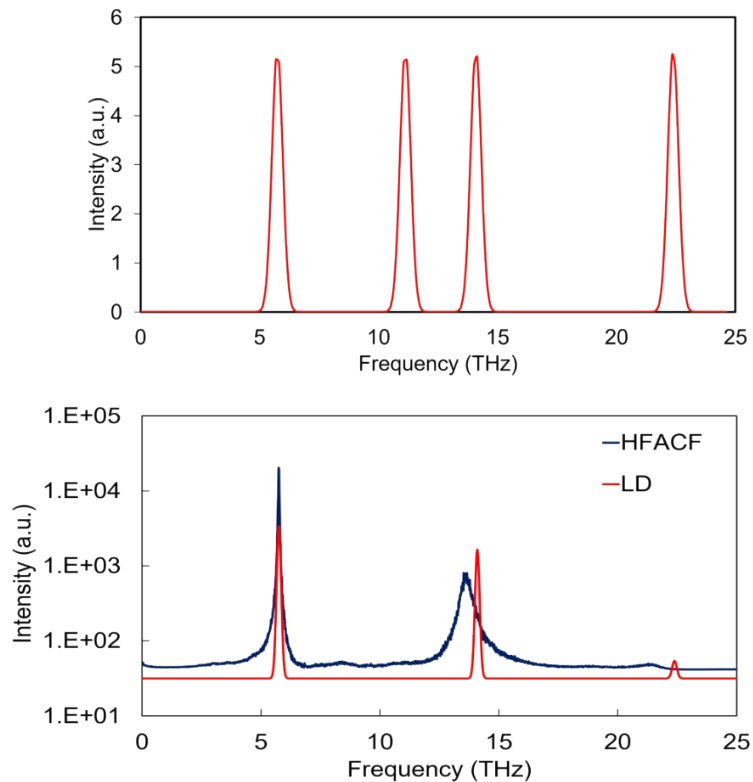


**Figure S13.** Untreated phonon density of states (PDOS) of bulk SrTiO<sub>3</sub> at the gamma point (top). Treated PDOS compared with the HFACF spectrum (Log10 scale) at 300K for bulk SrTiO<sub>3</sub> (bottom). The PDOS of SrTiO<sub>3</sub> would contains four Longitudinal Optical Modes (LO) at the  $\Gamma$  point although as stated in the Methodology, one is removed as its vibration is associated with a zero net change in momentum and therefore the mode will not either be associated with a net change in heat-flux or in dipole moment (IR inactive mode).

## References

- 1 M. S. Green, *J. Chem. Phys.*, 1954, **22**, 398-413.
- 2 R. Kubo, *J. Phys. Soc. Jpn.*, 1957, **12**, 570-586.
- 3 S. Plimpton, *J Comput. Phys.*, 1995, **117**, 1-19.
- 4 D. P. Sellan, E. S. Landry, J. E. Turney, A. J. H. McGaughey and C. H. Amon, *Phys. Rev. B*, 2010, **81**, 214305.
- 5 A. J. H. McGaughey and J. M. Larkin, *Ann. Rev. Heat Transfer*, 2014, **17**, 49-87.
- 6 A. J. H. McGaughey and M. J. Kaviany, *Ann Arbor*, 2002, **1001**, 48109-42125.
- 7 A. J. H. McGaughey and M. Kaviany, *Int. J. Heat Mass Transfer*, 2004, **47**, 1799-1816.
- 8 A. Togo, F. Oba and I. Tanaka, *Phys. Rev. B*, 2008, **78**, 134106.
- 9 A. Togo, L. Chaput and I. Tanaka, *Phys. Rev. B*, 2015, **91**, 094306.
- 10 E. S. Landry, M. I. Hussein and A. J. H. McGaughey, *Phys. Rev. B*, 2008, **77**, 184302.
- 11 A. J. H. McGaughey, M. I. Hussein, E. S. Landry, M. Kaviany and G. M. Hulbert, *Phys. Rev. B*, 2006, **74**, 104304.
- 12 P. Canepa, PhD Thesis, University of Kent, 2012.
- 13 D. de Ligny and P. Richet, *Phys. Rev. B*, 1996, **53**, 3013-3022.